

# A Sepic Type Switched Mode Power Supply System For Battery Charging In An Electric Tricycle (Auto-Rickshaw)

Kureve, D.T., Igwue, G.A, Goshwe, N.Y

**Abstract:** This paper analyzes the plug-in electric tricycle (Auto rickshaw) battery charging system using a non-isolated DC-DC SEPIC converter which operates as a switched mode power supply (SMPS). The control of dc voltage output is by varying the gating pulses duty cycle of the switch in the dc-dc converter using PID controller based PWM technique. The 60 V, 30 A DC-DC SEPIC converter is designed to provide non-inverting voltage buck from the rectified AC mains for charging deep cycle battery bank in an electric auto rickshaw. The charger system is implemented using MATLAB/Simulink.

**Index Terms:** SMPS, AC mains, Electric tricycle (Auto rickshaw), PID Controller, PWM, SEPIC converter, MATLAB/Simulink

## 1 INTRODUCTION

Switched mode power supplies (SMPS) are extensively used in charging batteries [2]. Designing high performance battery chargers using DC-DC non-isolated power converters with low cost, small size, and high efficiency makes it a challenge due to the electro-magnetic interference (EMI) [3]. The design becomes more difficult for applications that demand high voltage gains with low input and output current ripple [2]. The single-ended primary inductor converter (SEPIC) is a DC-DC voltage converter that is able to boost or buck a dc input voltage. One of the merits of a SEPIC converter is its non inversion of the output voltage unlike the buck-boost converter; it also offers easy implementation of magnetic coupling [5-7]. But they usually suffer from higher switch voltage stresses and their control can be complex, due to the two pairs of undamped complex poles in its duty cycle to output voltage gain [4-6]. Lithium-ion battery use in plug-in electric vehicle battery technologies has been high due to its high power density and good depth of discharge but its high cost has made it a reason why Electric Vehicles (Evs) are expensive and not affordable. The Lead acid battery is cheap, affordable and easily available for use especially in developing countries where cost is a major factor in making purchase decisions [8-10]. A wide voltage range of the on-board charger is mapped to a wide voltage range of Lead acid cell [9]. The charging profile of a lead acid battery is as shown in Figure 1.

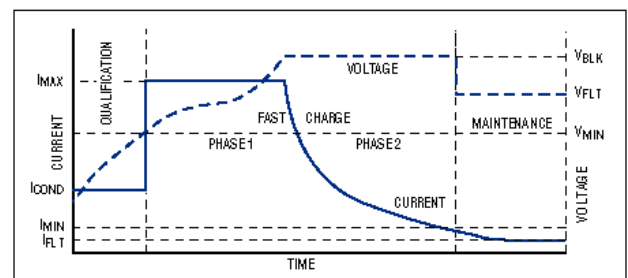


Figure 1: Lead acid battery charging profile

The battery charging stages of any typical lead acid value regulated lead acid (VRLA) battery include [3-6]; i. Trickle charge ii. Bulk charge iii. Absorption charge iv. Float charge. This paper implements a 60 V, 30 A SMPS system using a non-isolated SEPIC converter which is used to charge the 48 V battery bank of an electric tricycle (electric auto rickshaw) using MATLAB/Simulink software.

## 2. RESEARCH METHOD

One of the methods for improving low power factor is to install a SEPIC converter as a power factor corrector. The SEPIC converter is connected to a AC-DC rectifier as presented in Figure 2.

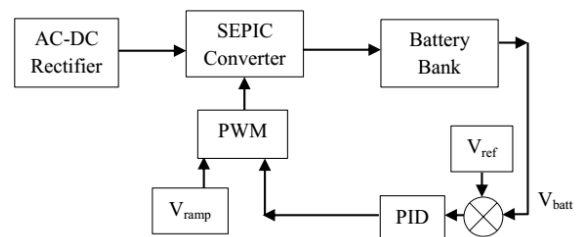


Figure 2: Block diagram of the system

From Figure 2, the reference voltage  $V_{ref}$  is compared with the output voltage of the SEPIC converter, the error is fed into a tuned PID controller circuit which is then compared with a ramp voltage to produce the gating pulses needed to switch the power MOSFET. A SEPIC DC-DC converter consist of two inductors ( $L_1$  and  $L_2$ ), two capacitors ( $C_1$  and

- Kureve, D. T is currently pursuing a PhD program in Power Electronics Engineering at University of Agriculture, Makurdi, Benue State, Nigeria, PH-+2348155613249. E-mail: [kurevedt@gmail.com](mailto:kurevedt@gmail.com)
- Igwue, G. A is currently a Professor of Communication Engineering at University of Agriculture, Makurdi, Benue State, Nigeria, PH-+2348080127327. E-mail: [gaigwue@yahoo.com](mailto:gaigwue@yahoo.com)
- Goshwe, N. Y is currently an Associate Professor of Power Electronics Engineering at University of Agriculture, Makurdi, Benue State, Nigeria, PH-+2348077451555. E-mail: [nentawe@gmail.com](mailto:nentawe@gmail.com)

$C_o$ ), a diode ( $D_1$ ) and switch (Q) which is typically a transistor such as MOSFET.

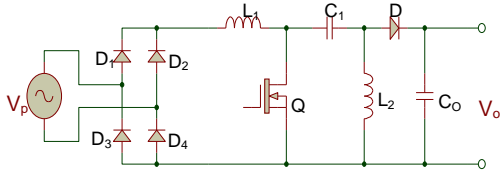


Figure 3: The circuit diagram of the SEPIC.

The SEPIC converter in Figure 3 is in Continuous Conduction Mode (CCM) therefore, current in the inductor  $L_1$  is always greater than zero.

### 3. DESIGN ANALYSIS

#### 3.1 DC analysis

During switch ON: From Figure 3, when the switch (Q) is ON, the voltage across both inductors is equal to  $V_p$  and capacitor  $C_1$  and inductor  $L_2$  are connected in parallel. The Diode  $D_1$  is reverse bias, and the load current is supplied by capacitor  $C_o$ .

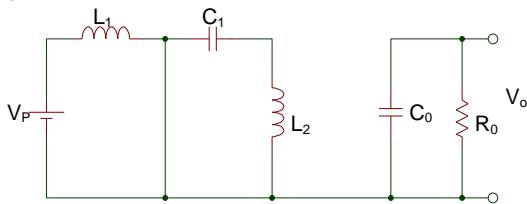


Figure 4: Equivalent circuit of the SEPIC when Q is ON.

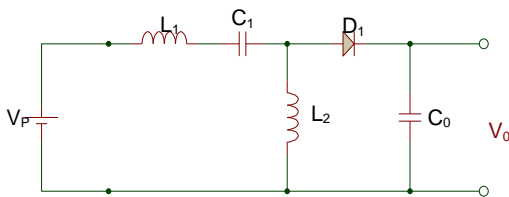


Figure 5: Equivalent circuit of the SEPIC when Q is OFF

When the power switch Q is OFF, capacitor  $C_1$  is charged via the inductor  $L_1$  and inductor  $L_2$  supplies the output current to the load as shown in Figure 5. Summing the average currents using KCL in Figure 5.

$$I_{D1} = I_{L1} - I_{L2} \tag{1}$$

When Q turned ON, let  $T$  = Switching Period,  $f_{sw}$  = Switching Frequency,  $t_{on}$  = Switch ON time,  $t_{off}$  = Switch OFF time,  $D$  = Duty cycle, Applying KVL with reference to  $L_1$ , Since,  $V_o = V_{C2}$

$$I_{L1} = \frac{V_p - V_{C1} - V_o}{L_2} \times t_{off} \tag{2}$$

$$I_{L2} = \frac{-V_o}{L_2} \times t_{off} \tag{3}$$

Average Voltage across  $L_1$  &  $L_2$  is zero, therefore,

$$V_p - V_{L1} - V_{C1} - V_{L2} = 0 \tag{4}$$

Voltage across the coupling capacitor ( $C_1$ ) is equal to  $V_p$ , as the capacitance of  $C_o$  is adequate to supply output current when the switch is ON.

$$V_p = V_{C1} \tag{5}$$

Substituting equation (5) into equation (2) we have

$$I_{L1} = \frac{-V_o}{L_1} \times t_{off} \tag{6}$$

Averaging the equations (2) & (3) to zero,

$$\begin{aligned} \frac{V_p}{L_1} \times t_{on} - \frac{V_o}{L_1} \times t_{off} &= 0 \\ V_p \times t_{on} &= V_o \times t_{off} \end{aligned}$$

But  $t_{on} = DT$ , and  $t_{off} = (1 - D)T$

Substituting in  $t_{on}$  and  $t_{off}$ , we shall have the expression as:

$$V_p \times DT = V_o \times (1 - D)T, \tag{7}$$

$V_o/V_p$  is the transfer function of the SEPIC converter in continuous mode as:  $\frac{V_o}{V_p} = \frac{D}{1-D}$

Duty cycle consideration: The duty cycle  $D$  in terms of voltage, of a SEPIC converter operated in CCM is given as:

$$D = \frac{V_o}{V_p + V_o} \tag{8}$$

Duty cycle  $D$  maximum and minimum values are:

$$D_{max} = \frac{60}{50+60} = 0.55 \text{ and } D_{min} = \frac{60}{340+60} = 0.15$$

#### 3.2 Selection of SEPIC Power Components

The components for the SEPIC converter are:

##### Inductor Selection:

The inductors are wound on the same core, thus the inductance is given by:

$$L_1 = L_2 \geq \frac{V_p(\min) \times D_{max}}{2 \times \Delta I_L \times f_{sw}} \geq \frac{50 \times 0.55}{2 \times 5.24 \times 200 \times 10^3} \geq 26.24 \mu H$$

For inductor ripple current for  $L_1$  is:

$$\Delta I_L = \frac{I_o \times (V_o + V_{D1})}{V_p(\min) \times \eta} \times 30\% = \frac{30 \times (60 + 0.5)}{50 \times 0.9} \times 30\% = 12.1 A$$

Peak inductor current for  $L_1$  is:

$$I_{L1(\text{peak})} = \frac{I_o \times (V_o + V_{D1})}{V_p(\min) \times \eta} \times \left\{ 1 + \frac{30\%}{2} \right\} = \frac{30 \times (60 + 0.5)}{50 \times 0.9} \times \left\{ 1 + \frac{30\%}{2} \right\} = 46.38 A$$

Peak inductor current for  $L_2$  is:

$$I_{L2(\text{peak})} = I_o + \frac{\Delta I_L}{2} = 30 + \frac{12.1}{2} = 36.05 A$$

**Capacitor selection:**

The input coupling capacitor of the SEPIC converter is chosen as 10 μF.

**Output capacitor selection:**

Assuming the peak-to-peak ripple is 2-5% of the output voltage, then:

$$C_o \geq \frac{I_o}{0.5 \times \Delta V_{ripple}} \times \frac{D_{max}}{f_{sw}} \geq \frac{30}{0.02 \times 60 \times 0.5} \times \frac{0.55}{200 \times 10^3} \geq 137.5 \times 10^{-6} \geq 137.5 \mu F$$

**Power Mosfet Selection**

Mosfet peak current is:

$$I_{Q1(peak)} = I_{L1(peak)} + I_{L2(peak)} = 46.38 + 36.05 = 82.43 A$$

And R.M.S current value is:

$$I_{Q1(rms)} = I_o \times \sqrt{\frac{V_o + V_D}{V_{in(min)}}} = 30 \times \sqrt{\frac{60 + 0.5}{50}} = 33 A$$

The open loop transfer function of the SEPIC converter can be expressed as:

$$D = 0.55, L_1 = L_2 = 26.24 \mu H, C_1 = 10 \mu F, C_o = 220 \mu F, R = 1.2 \Omega, V_p = 340 V$$

$$\frac{V_o(s)}{d(s)} = 1679.0 \times \frac{-s^3 + 6.635 \times 10^9 s^2 - 30.33 s + 1.475 \times 10^{13}}{s^4 + 3788000 s^3 + 3.055 \times 10^8 s^2 + 5.209 \times 10^{11} s + 3.072 \times 10^{16}}$$

**3.3 Simulation Study**

The simulation of the PID controlled SMPS used for charging a battery bank is done in MATLAB/Simulink. The simulation parameters are as presented in Table

**Table 6: SEPIC DC-DC Converter design specifications:**

| Description           | Value   |
|-----------------------|---------|
| Minimum Input voltage | 50 V    |
| Maximum Input voltage | 340 V   |
| Switching frequency   | 200 kHz |
| Output current        | 30 A    |
| Output voltage        | 60 V    |
| Efficiency (η)        | 90 %    |

The simulation is done in the Simulink environment of MATLAB software and the circuit is as presented in Figure 6

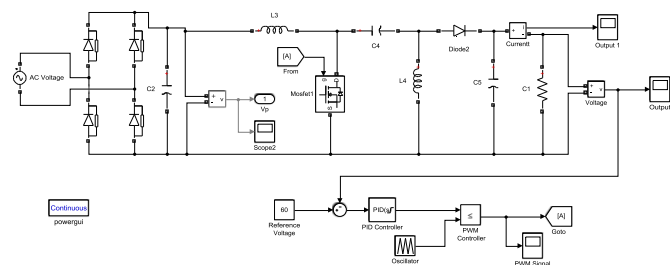


**Figure 6: Simulink model of the SEPIC Converter with PID controller feedback control.**

**4.0 RESULTS**

This chapter presents output obtained from the simulations of analysis done in chapter three.

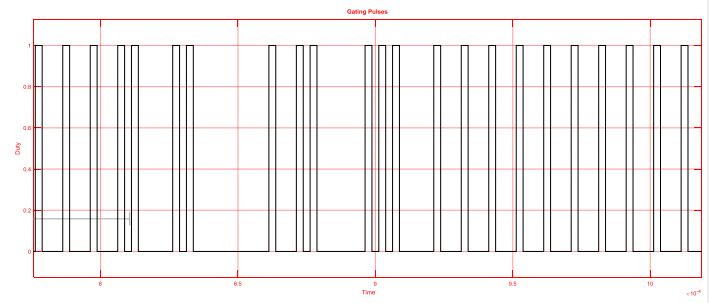


**Figure 7: PWM Gating pulses**

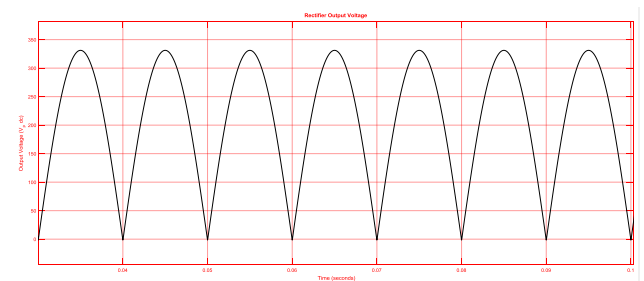


**Figure 8: 240 Vrms to 339 Vdc AC-DC rectified Voltage on load**

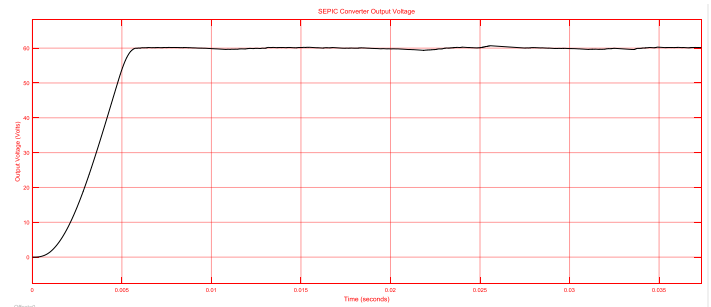


**Figure 9: Output Voltage of SEPIC converter with PID control**

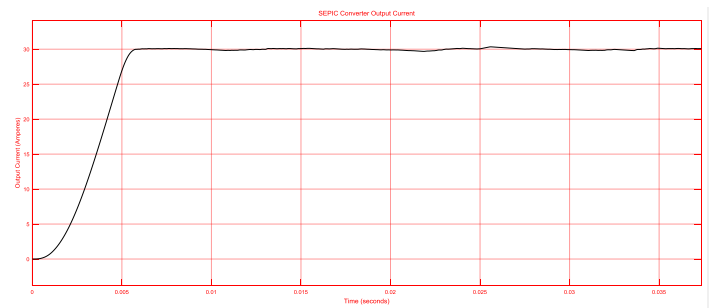


**Figure 10: Output current of the SEPIC converter with PID control**

Figure 7 depicts the PWM gating pulses used to switching the power Mosfet on and off. Figure 8 represents the output voltage of the rectifier on no-load of a 240 Vrms AC main indicates 339 V dc rectified voltage with ripples without filtering. Figure 9 represents the output voltage of 60 V for the SEPIC converter with PID controller feedback control from AC mains. Figure 10 represents the current output from the SMPS PID controlled SEPIC converter.

## 5.0 CONCLUSION

This paper presents a battery charging circuit using SEPIC converter which can be used for charging lead acid battery bank in an electric tricycle. From the results presented in Figures 6-10, the PWM pulses are determined by the PID controller via the error from the difference of the set voltage and output voltage. Also the output dc voltage of the SEPIC converter is 60 V and the output current is 30 A.

## REFERENCES

- [1]. Chun T. Rim, Gyu B. Joung, and Gyu H. Cho, "Practical Switch Based State-Space Modeling of DC-DC Converters with All Parasitics," IEEE Trans. on power electronics, vol. 6 No. 4 October 1991
- [2]. Dhanasekaran S., E.Sowdesh Kumar, R.Vijaybalaji, (2014). "Different Methods of Control Mode in Switch Mode Power Supply- A Comparison", International Journal of Advanced Research in Electrical, Electronics and Instrumentation Engineering (IJAREEIE), Vol. 3, Issue 1, pp. 6717-6724.
- [3]. Ali Davoudi and Juri Jatskevich, "Parasitics Realization in State-Space Average-Value Modeling of PWM DC-DC Converters Using an Equal Area Method," IEEE Tran. On circuits and systems-I: regular papers, vol. 54, No. 9, September.
- [4]. S. Ben-Yaakov, D. Adar and G. Rahav, A SPICE compatible Behavioral Model of SEPIC Converters, IEEE PESC'96, Vol. 2, pp. 1668- 1673
- [5]. W. M. Moussa, Modeling and performance evaluation of a DC/DC SEPIC converter, APEC'95, Vol. 2, pp. 702-706
- [6]. D. Adar, G. Rahav and S. Ben-Yaakov, A unified behavioral average model of SEPIC converters with coupled inductors, IEEE PESC'97, Vol. 1, pp. 441- 446
- [7]. H. Wang and A. Khaligh, "Comprehensive topological analyses of isolated resonant converters in PEV battery charging applications," in IEEE Transportation Electrification Conference and Expo.pp.1-7, 2013.
- [8]. A. Khaligh and S. Dusmez, "Comprehensive Topological Analysis of Conductive and Inductive Charging Solutions for Plug-In Electric Vehicles," IEEE Trans. Veh. Technol., vol. 61, no. 8, pp. 3475-3489, Oct. 2012.
- [9]. M. Yilmaz and P. Krein, "Review of Battery Charger Topologies, Charging Power Levels and Infrastructure for Plug-in Electric and Hybrid Vehicles," IEEE Trans. Power Electron., vol. 28, pp. 1-1, 2012.
- [10]. G. Pellegrino, E. Armando, and P. Guglielmi, "An Integral Battery Charger With Power Factor Correction for Electric Scooter," IEEE Trans. Power Electron., vol. 25, no. 3, pp. 751-759, Mar. 2010.